Argon treatment alters microglial activation and neuronal cell death after experimental subarachnoid hemorrhage – a randomized controlled animal trial

Benedikt Kremer
Rheinisch-Westfalische Technische Hochschule Aachen
Mark Coburn
Rheinisch-Westfalische Technische Hochschule Aachen
Agnieszka Weinandy
Rheinisch-Westfalische Technische Hochschule Aachen
Kay Nolte
Rheinisch-Westfalische Technische Hochschule Aachen
Hans Clusmann
Rheinisch-Westfalische Technische Hochschule Aachen
Michael Veldeman
Rheinisch-Westfalische Technische Hochschule Aachen
Anke Höllig (ahoellig@ukaachen.de)
Rheinisch-Westfalische Technische Hochschule Aachen https://orcid.org/0000-0001-6798-5703

Research article

Keywords: argon, neuroprotection, neuroinflammation, subarachnoid hemorrhage, microglial activation

Posted Date: September 3rd, 2019

DOI: https://doi.org/10.21203/rs.2.11832/v1

Abstract

Background Here, we demonstrate argon´s neuroprotective and immunomodulatory properties after experimental subarachnoid hemorrhage (SAH) examining various localizations (hippocampal and cortical regions) with respect to neuronal damage and microglial activation 6, 24 and 72h after SAH. Methods One hour after SAH (endovascular perforation rat model) or sham surgery, a gas mixture containing 50 vol% argon (argon group) or 50 vol% nitrogen (control group) was applied for 1h. Cerebral coronal sections (H&E; Iba-1 stained) were analyzed for neuronal cell death and microglial activation in predefined anatomical regions. Results Comparing the hippocampal regions 6h after SAH reduced neuronal damage was seen in the argon group ($p<0.0001$) as well as in the cortical region ($p=0.014$). Over time the effect diminished: A substantial difference 24h after SAH was only seen for the cortical region ($p=0.004$). No significant difference was observed 72h after SAH. The hippocampal and overall microglial activation 24h after SAH were significantly reduced in the argon group ($p=0.013$; $p<0.0001$), whereas 72h after SAH significance was only detected in the cortical area ($p=0.014$). Conclusion Argon treatment ameliorated early neuronal damage after SAH. However, inhibition of microglial activation might indicate a beneficial effect with regard to secondary inflammatory.

Background

Subarachnoid hemorrhage (SAH) is a less common subtype of stroke accounting for about 5% of all of the stroke cases (1). Patients suffering from SAH are usually younger than those affected by ischemic stroke (2). Nevertheless, the case fatality after SAH is around 50% and .the mortality rates of the survivors are enormous (indicated by a standardized mortality ratios of 1.7 (95% CI 1.4 to 2.1) overall and 3.2 (95% CI 0.8 to 13.1) for patients<40 years) (3).

Spontaneous subarachnoid hemorrhage is usually caused by the rupture of a cerebral aneurysm (4). The rupture of an intracranial aneurysm causes a sudden impact with arterial pressure into the subarachnoid space. This results in a sudden increase of the intracranial pressure, in a short-term global ischemia and in a destruction of the blood-brain barrier.

The damaging mechanisms in the first 72 hours after the event of bleeding are summarized under the term early brain injury (EBI) (5). The extent of damage within this timeframe also determines the likelihood of secondary damage such as delayed cerebral ischemia, which is a major cause of secondary mortality and morbidity and still comprises an entity difficult to treat (6). So far, no specific therapeutic options for the treatment of EBI have been established in clinical practice.

Argon is an inert noble gas, it is not chemically reactive, thus it easily overcomes the blood-brain barrier. However, it shows biological effects, in particular neuroprotective effects, which could be detected in previous studies. The exact mechanism behind these effects and their temporal dynamics is not yet clear (7, 8).

Using in vitro experiments with organotypic hippocampus sections, these neuroprotective effects could be demonstrated both in a model of traumatic brain injury and in an ischemic model with oxygen and glucose deprivation (9).

In vivo, this neuroprotective effect also has been confirmed in the middle cerebral artery occlusion (MCAO) ischemia model (10, 11) and, later on, also for the SAH model showing a decreased neuronal damage in the hippocampal region for the argon treated animals (12). Both neuroprotective effects as well as reduction of the secondary inflammation in terms of microglial activation have also been demonstrated for xenon treatment after experimental SAH (13). However, argon has distinct advantages over xenon applied as a therapeutic. It does not show any narcotic effects and it is financially more cost-effective, which makes subsequent use much more realistic.

We therefore aim to analyze the neuroprotective effect of argon after experimental SAH depending on time after SAH as well as localization examining various cortical and hippocampal regions of interest in order to depict a more detailed and accurate patterns of the effects after treatment with argon. Further, the influence of argon on the delayed activation of microglia determining to a major extent secondary injury will be examined.

Methods

Study Design

We performed a randomized controlled animal trial examining the neuroprotective effects of argon inhalation (50 vol% for 1 h) with treatment initiation 1 h after SAH induction. Three observation times were applied resulting in a total of 12 groups. Parts of this study are already published elsewhere (12).

Ethical Statement

All of the experiments were conducted in accordance with the Guide for Care and Use of Laboratory Animals (National Research Council, and the Committee for the Update of the Guide for the Care and Use of laboratory Animals; 8th edition 2011).The study protocol was approved by the government agency for animal use and protection (Protocol number: TVA 10416G1 approved by “Landesamt für Natur, Umwelt und Verbraucherschutz NRW,” Recklinghausen, Germany). “The Animal Research: Reporting of In Vivo Experiments guidelines” (14) were used as criteria for adequate performance and reporting of experiments.

Animals

Male Sprague-Dawley rats (body weight 300 – 400 g, Charles River, Sulzfeld, Germany) were used for the experiments. They were housed for at least 1 week before the beginning of the experiments with provided food in a specific pathogen-free environment maintaining a 12-h light/dark cycle. Before starting the

experiments the animals were first randomized by drawing a lot to a Sham or a SAH group. The experimental groups were defined as follows: Sham N_2 (Sham surgery after 1 h delay followed by ventilation with 50 vol% O_2/50 vol% N_2 for 1 h), Sham Ar (Sham surgery after 1 h delay followed by ventilation with 50 vol% O_2/50 vol% Ar for 1 h), SAH N_2 (SAH induction after 1 h delay followed by ventilation with 50 vol% O_2/50 vol% N_2 for 1 h), and SAH Ar (SAH induction after 1 h delay followed by ventilation with 50 vol% O_2/50 vol% Xe for 1 h) (see Results section, Figure 1).

Experimental Procedure

To induce SAH we used the modified endovascular perforation model (15, 16). During the entire procedure ICP and CBF were monitored.

Anesthesia was induced by intraperitoneal injection of a mixture of midazolam (2 mg/kg), medetomidine (0.15 mg/kg), and fentanyl (0.0075 mg/kg) (17). A quarter of the initial dosage was injected in 30–45 min intervals to maintain anesthesia. Postoperative analgesia was started directly after surgery via intramuscular injection of metamizole (20 mg/kg) and continued until euthanasia (6, 24 or 72 h after SAH induction). Body temperature was maintained at 37°C via a heating pad (Physitemp Instruments, Inc., Clifton, NJ, USA). Two laser Doppler flowmetry probes were fixated in proximity of the bregma to measure regional cerebral blood flow (rCBF) (Moor Instruments, Axminster, Devon, UK). A left side parietal ICP probe was inserted for continuous ICP monitoring (Microsensor/Codman ICP Express Monitor, Codman/De Puy, Raynham, MA, USA). SAH was induced by the modified endovascular perforation model initially described by Park et al (15) After exposing the left common carotid artery, the left internal carotid artery (ICA) was identified and a tube containing a wolfram wire was advanced intravascularly. Perforation of the vessel was performed via advancement of the wire and subsequent SAH was verified by a sudden increase in ICP and a bilateral decrease in rCBF. Sham-operated animals underwent the same anesthesia and surgical procedure, but the wire was advanced into the ICA without perforation of the vessel.

One hour after SAH induction or Sham surgery, the animals were ventilated for 1 h with either a mixture of 50 vol% O_2/50 vol% argon (Air Liquide, Paris, France) or 50 vol% O_2/50 vol% N_2 (control group). Euthanasia was performed 6, 24 or 72 h after SAH induction by exsanguination under deep anesthesia followed by decapitation. Brains were harvested and cut into 2 mm coronal slices, fixated in paraformaldehyde, and embedded in paraffin.

Histology/Immunohistochemistry

Paraffin embedded brain slices were cut in 2µm thick sections. After placing the sections on silane-coated slides they were deparaffined. One section was routinely hematoxylin/eosin (H&E) stained. Two

consecutive sections were de-waxed, rehydrated, and heated in citrate buffer for antigen retrieval. After blocking of non-specific binding by incubation in PBS containing 2% normal goat serum, one slide per animal was incubated with anti-Iba-1 (1:500; Wako Chemicals, Neuss, Germany) as primary antibody diluted in blocking solution . Appropriate biotinylated secondary antibodies were used (1:200, Vector Laboratories Ltd., Peterborough, UK) for 15 min.

Neuronal Cell Damage

H&E sections were made to assess neuronal damage. Nine regions of interest were defined (five hippocampal regions: CA1, CA2, CA2/3, CA3, and dentate gyrus and four cortical regions: S1, Pir, PLCo and PMCo; selected according to “The Rat Brain in Stereotaxic Coordinates” by Paxinos/Watson (18)). These regions were counted in a standardized fashion using a 400-fold magnification, photographed with an Axioplan microscope (ZEISS, Germany). and neuronal death according to anatomical hallmarks such as hypereosinophilia, shrunken cytoplasm and pyknotic nuclei was quantified. This counting process was done three times by a single investigator blinded to treatment allocation.

Microglial Activation

For the evaluation of the microglial activation, sections were stained with the antibody against Iba-1. Here, the microglia activation was quantified in the known 9 regions of interest (five in the hippocampal regions: CA1, CA2, CA2/3, CA3, and dentate gyrus and four cortical regions: S1, Pir, PLCo and PMCo) and in the corpus callosum (CC) as a representative of the white matter.

An absolute microglial cell count was performed in a similar fashion in the Iba-1 (ionized calcium-binding adapter molecule 1) stained sections. The five hippocampal, the four cortical regions of interest and the corpus callosum as a region of interest per animal were photographed. The absolute number of activated Iba-1-positive cells was software-assisted counted out in the CA1, CA2, CA2/3, CA3, DG, S1, Pir, PLCo, PMCo of the left hemisphere and also in the Corpus callosum.

Experimental Outcomes

The primary outcome was left side neuronal damage. The secondary outcome was microglial activation.

Statistical Methods

Sample size calculation was extrapolated from previous studies (12, 13) resulting in an estimated sample size of n =7 per treatment group (effect size estimation according to the results of neuronal damage after SAH and xenon treatment for CA3 = 1.02). A alpha-error of 0.1 and beta of 0.7 was presumed, thus resulting in the calculated sample size (G*Power 3.9.1.2 downloaded at http://www.gpower.hhu.de/). All statistical analyses were performed using SPSS v 25.0 (SPSS Inc., Chicago, IL, USA). All graphics were acquired using GraphPad Prism (GraphPad Software Inc., La Jolla, CA, USA). A *p*-value of <0.05 was considered statistically significant.

For statistical analysis dependent on normality testing (Kolmogorov–Smirnov test), unpaired t-test or Mann-Whitney U test were applied.

All data are presented as means ± SD unless stated otherwise.

Results

Baseline Data

A total of 83 animals have been analyzed. One animal had to be excluded due to premature death (not fulfilling the initially planned observation period), six animals in the Sham group had to be excluded due to tissue damage caused by CBF (cerebral blood flow) probes, 10 animals had to be excluded as the hippocampal region was not properly depicted in the available brain slices. Finally, 66 animals were included (see Flowchart, Fig. 1).

During the induction of SAH the peak intracranial pressure (ICP) was documented. In the argon group the mean ICP was significantly higher than in the control group (79.6 ± 18.7 vs. 62.3 ± 24.0; p < 0.03; unpaired t-Test) indicating a severer bleeding in the argon treated group (Fig. 2). No adverse events due to argon administration have been detected.

Neuronal Cell Damage in H&E-Stained Sections

Neuronal cell death was quantified using hematoxylin and eosin stained section based on anatomical hallmarks such as hypereosinophilia, shrunken cytoplasm and pyknotic nuclei. Hippocampal and cortical ROIs were defined according to the anatomical landmarks (see Fig. 3) and apoptotic neurons per ROI were counted indicating neuronal damage.

The detailed analyses are shown in Tables 1 – 3 (see Supplementary Material).

Summing up the results for the specific regions 6 h after SAH a significantly less damage in the hippocampus was seen in the argon treated group (p < 0.0001; Mann Whitney U), which 24 h and 72 h after SAH was no more detectable (p = 0.192; p = 0.215: Mann Whitney U). With regard to the cortical

ROIs the sum score differed significantly (less damage in the argon group) at 6 and 24 h after SAH ($p = 0.014$; $p = 0.004$; Mann Whitney U). Similarly the overall result (summing up all the counted regions) showed a significantly reduced neuronal damage at 6 and 24 h after SAH ($p < 0.0001$; $p = 0.001$; Mann Whitney U). However, both sum scores showed no more difference 72 h after SAH. The sum score including the results for the Sham animals are demonstrated in Figure 4.

Microglial Activation in Iba-1 Stained Sections

Ionized calcium-binding adapter molecule 1 (Iba-1) is a protein expressed in the cytoplasm, which is highly specific for microglia. Activation of microglia is associated with increase of Iba-1 expression (19, 20). Therefore, Iba-1 expression has been used as a surrogate marker for microglia activation. We analyzed the Iba-1 positive cells presenting a microglial habitus in ten ROIs (five hippocampal regions, four cortical regions and the corpus callosum) in order to identify the effect of argon treatment on secondary inflammatory reaction after SAH. Iba-1-positive cells were software-assisted quantified in a HPF, focusing on the center of each ROI.

In the early phase after SAH (6 h) no significant difference with regard to microglia activation was seen most probably due to the time-dependent activation of microglia with a peak around two days after injury. Detailed results for each ROI are displayed in Tables 4 -6 (see Supplementary Material). Microglial activation differed most distinctly between the treatment groups at 24 h after SAH (hippocampal, cortical and overall sum scores showed a significant difference; $p = 0.013$; $p = 0.060$; $p < 0.0001$; Mann Whitney U), whereas 72 h after SAH the difference was only seen for the cortical sum score ($p = 0.014$; Mann Whitney U). The sum scores are illustrated in Figure 5.

Discussion

Here, we demonstrate the effect of argon administration after experimental SAH on neuronal cell death and microglial activation.

Microglia plays a major role in the pro-inflammatory cytotoxic response and participates in the immunosuppressive processes contributing to further tissue damage (21). Reduction of microglial activation may attenuate secondary damage due to EBI. There is data from human specimen confirming this hypothesis: A causal link between microglia accumulation and neuronal cell death has been proposed (22). However, microglial activation may represent both devastating but also beneficial properties depending on its polarization (23). Thus, microglia might play a biphasic action due to its polarization state. However, it has been argued that the concept of microglial polarization depicts a black and white pattern which does not properly reflect the physiological smooth transition or even coexistence

of both states (24). It becomes even more complex if the multiple interactions of microglia with other cell types and possible communication via various pathways are taken into account (25).

Here, we demonstrate a time-dependent activation pattern after experimental SAH, which is influenced by argon treatment and affects also remote, white matter locations such as the corpus callosum. In contrast to our previously published data on xenon treatment after experimental SAH (13) our currently published data are more heterogeneous and more difficult to interpret. Thus, especially concerning the specific localizations the data has to be confirmed examining a larger sample size whereas the pooled data (with increased sample size by accumulating different regions within one larger area) may represent an actual effect.

Our primary outcome, neuronal cell death after SAH was influenced by argon treatment especially 6 and 24 h after SAH. This is in line with multiple studies demonstrating a neuroprotective effect by argon treatment such after experimental stroke, SAH but also after cardiac arrest (26). However we were not able to confirm the previously stated effect on the neuronal survival of the dentate gyrus (12) as the protective effects seen here are rather located in other hippocampal areas but not the dentate gyrus. Further, the effect of reduced neuronal cell death diminishes with time, which may also represent a lack of sustainability of the argon treatment. Thus, future strategies should evaluate a more longer application of the noble gas. However, there is also controversial data on argon´s proposed neuroprotective action: Using a rodent model for cardiac arrest neither neurological nor histological improvement by argon recently could be shown (27). Thus, larger multicentric experimental and maybe in the future clinical trials have to be conducted to elucidate the potential of argon treatment.

Limitations

The relatively small number of cases in the individual groups, in particular in the Sham groups (as low as n = 2), but also treatment groups (not reaching estimated sample size) is a main limitation. Due to technical issues (e.g. insufficient quality of sections) animals had to be excluded resulting in small sample size. Further, animals were treated within the framework of a controlled randomized study but analyses were performed later on. Thus, further inclusion of animals was not possible anymore resulting in the mentioned small sample sizes.

Additionally, sections were analyzed by one individual which was blinded for the treatment. A bias derived by subjective interpretation is possible.

Further, no double staining to identify microglia has been performed. Iba-1 is a robust but not a specific marker for microglia. Further, no distinct NeuN staining to detect vital neurons has been carried out. Cell death has been quantified by morphological means.

Finally, there is a slight trend without statistical significance ($p = 0.2559$; $p = 0.3186$) towards an increased neuronal damage in the Sham argon group compared to Sham N2 at 6 and 24 h after SAH.

This may be due to small sample size and represent a sampling bias (especially in the Sham argon group; n = 2 respectively n = 5), however, it cannot be excluded that argon comprises a injury specific neuroprotective action.

Conclusion

The pattern of neuronal damage after experimental SAH is modified by argon treatment resulting in an early decrease of neuronal damage, which –unfortunately- is not sustainable. Microglial activation is distinctly reduced in the argon treated group.

Abbreviations

SAH, subarachnoid hemorrhage; ICP, intracranial pressure; rCBF, regional cerebral blood flow; ROI, region of interest; ICA, internal carotid artery; HPF, high power field; Ar, argon; N2, nitrogen; CA1: cornu ammonis 1; CA2: cornu ammonis 2; CA2/3: cornu ammonis 2/3; CA3: cornu ammonis 3; DG: dentate gyrus; S1: primary somatosensory cortex; Pir: piriform cortex; PLCo: postero-lateral cortex; PMCo: postero-medial cortex

Declarations

Author Contributions

Animal experiments: AH. Data analysis: BK and AH. Manuscript drafting: BK. Support for histopathological examinations: KN, AW and MV. Manuscripts revision and editing: BK, MC, KN, AW, HC, MV, and AH. Final approval of the manuscript: BK, MC, KN, AW, HC, MV, and AH.

Conflict of Interest Statement

AH lectured for Air Liquide. MC consulted and lectured for Baxter Healthcare and Air Liquide. His institution received grant Support from the Deutsche Forschungsgemeinschaft (CO 799/9-1), Baxter Healthcare, and Air Liquide. All remaining authors have no potential conflict of interest to declare.

Funding

This trial was funded by the Start Program, RWTH Aachen. The funders had no role concerning study design, data collection and analysis, decision to publish, or preparation of the manuscript.

Acknowledgements

We like to thank Rosmarie Blaumeiser-Debarry and Birgit Nellessen for their support and technical assistance.

Availability of data and materials

Original data is available on request from the author.

Ethics approval and consent to participate

The study protocol was approved by the government agency for animal use and protection (Protocol number: TVA 10416G1 approved by “Landesamt für Natur, Umwelt und Verbraucherschutz NRW,” Recklinghausen, Germany).

References

1. van Gijn J, Kerr RS, Rinkel GJE. Subarachnoid haemorrhage. Lancet 2007; 369(9558):306–18.
2. Rooij NK de, Linn FHH, van der Plas JA, Algra A, Rinkel GJE. Incidence of subarachnoid haemorrhage: a systematic review with emphasis on region, age, gender and time trends. J Neurol Neurosurg Psychiatry 2007; 78(12):1365–72.
3. Wermer MJH, Greebe P, Algra A, Rinkel GJE. Long-term mortality and vascular event risk after aneurysmal subarachnoid haemorrhage. J Neurol Neurosurg Psychiatry 2009; 80(12):1399–401.
4. Macdonald RL, Schweizer TA. Spontaneous subarachnoid haemorrhage. The Lancet 2017; 389(10069):655–66.
5. Fujii M, Yan J, Rolland WB, Soejima Y, Caner B, Zhang JH. Early brain injury, an evolving frontier in subarachnoid hemorrhage research. Transl Stroke Res 2013; 4(4):432–46.
6. Veldeman M, Höllig A, Clusmann H, Stevanovic A, Rossaint R, Coburn M. Delayed cerebral ischaemia prevention and treatment after aneurysmal subarachnoid haemorrhage: a systematic review. Br J Anaesth 2016; 117(1):17–40.
7. Höllig A, Schug A, Fahlenkamp AV, Rossaint R, Coburn M. Argon: systematic review on neuro- and organoprotective properties of an "inert" gas. Int J Mol Sci 2014; 15(10):18175–96.
8. Ulbrich F, Goebel U. The Molecular Pathway of Argon-Mediated Neuroprotection. Int J Mol Sci 2016; 17(11).
9. Loetscher PD, Rossaint J, Rossaint R, Weis J, Fries M, Fahlenkamp A et al. Argon: neuroprotection in in vitro models of cerebral ischemia and traumatic brain injury. Crit Care 2009; 13(6):R206.
10. Ryang Y-M, Fahlenkamp AV, Rossaint R, Wesp D, Loetscher PD, Beyer C et al. Neuroprotective effects of argon in an in vivo model of transient middle cerebral artery occlusion in rats. Crit Care Med 2011; 39(6):1448–53.
11. Liu J, Nolte K, Brook G, Liebenstund L, Weinandy A, Höllig A et al. Post-stroke treatment with argon attenuated brain injury, reduced brain inflammation and enhanced M2 microglia/macrophage polarization: a randomized controlled animal study. Crit Care 2019; 23(1):198.
12. Höllig A, Weinandy A, Liu J, Clusmann H, Rossaint R, Coburn M. Beneficial Properties of Argon After Experimental Subarachnoid Hemorrhage: Early Treatment Reduces Mortality and Influences Hippocampal Protein Expression. Crit Care Med 2016; 44(7):e520-9.

13. Veldeman M, Coburn M, Rossaint R, Clusmann H, Nolte K, Kremer B et al. Xenon Reduces Neuronal Hippocampal Damage and Alters the Pattern of Microglial Activation after Experimental Subarachnoid Hemorrhage: A Randomized Controlled Animal Trial. Front Neurol 2017; 8:511.
14. Kilkenny C, Browne WJ, Cuthill IC, Emerson M, Altman DG. Improving bioscience research reporting: the ARRIVE guidelines for reporting animal research. PLoS Biol 2010; 8(6):e1000412.
15. Park I-S, Meno JR, Witt CE, Suttle TK, Chowdhary A, Nguyen T-S et al. Subarachnoid hemorrhage model in the rat: modification of the endovascular filament model. J Neurosci Methods 2008; 172(2):195–200.
16. Höllig A, Weinandy A, Nolte K, Clusmann H, Rossaint R, Coburn M. Experimental subarachnoid hemorrhage in rats: comparison of two endovascular perforation techniques with respect to success rate, confounding pathologies and early hippocampal tissue lesion pattern. PLoS ONE 2015; 10(4):e0123398.
17. Hockel K, Trabold R, Schöller K, Török E, Plesnila N. Impact of anesthesia on pathophysiology and mortality following subarachnoid hemorrhage in rats. Exp Transl Stroke Med 2012; 4(1):5.
18. Paxinos G, Watson C. Paxinos and Watson's the rat brain in stereotaxic coordinates. 7th ed. Amsterdam: Elsevier Acad. Press; 2014.
19. Imai Y, Ibata I, Ito D, Ohsawa K, Kohsaka S. A novel gene iba1 in the major histocompatibility complex class III region encoding an EF hand protein expressed in a monocytic lineage. Biochem Biophys Res Commun 1996; 224(3):855–62.
20. Vinet J, van Weering HRJ, Heinrich A, Kälin RE, Wegner A, Brouwer N et al. Neuroprotective function for ramified microglia in hippocampal excitotoxicity. J Neuroinflammation 2012; 9:27.
21. Perego C, Fumagalli S, Simoni M-G de. Temporal pattern of expression and colocalization of microglia/macrophage phenotype markers following brain ischemic injury in mice. J Neuroinflammation 2011; 8:174.
22. Schneider UC, Davids A-M, Brandenburg S, Müller A, Elke A, Magrini S et al. Microglia inflict delayed brain injury after subarachnoid hemorrhage. Acta Neuropathol 2015; 130(2):215–31.
23. Ma Y, Wang J, Wang Y, Yang G-Y. The biphasic function of microglia in ischemic stroke. Prog Neurobiol 2017; 157:247–72.
24. Ransohoff RM. A polarizing question: do M1 and M2 microglia exist? Nat Neurosci 2016; 19(8):987–91.
25. Kettenmann H, Hanisch U-K, Noda M, Verkhratsky A. Physiology of microglia. Physiol Rev 2011; 91(2):461–553.
26. Brücken A, Kurnaz P, Bleilevens C, Derwall M, Weis J, Nolte K et al. Dose dependent neuroprotection of the noble gas argon after cardiac arrest in rats is not mediated by K(ATP)-channel opening. Resuscitation 2014; 85(6):826–32.
27. Zuercher P, Springe D, Grandgirard D, Leib SL, Grossholz M, Jakob S et al. A randomized trial of the effects of the noble gases helium and argon on neuroprotection in a rodent cardiac arrest model. BMC Neurol 2016; 16:43.

Figure Legends

Figure 1:

Flowchart of the animals included.

Figure 2:

Peak ICP of the SAH treatment groups; given are mean and SD; * p<0.05

Figure 3.

Selected regions of interest. **(A)** In H&E staining, a high power field was focused on five regions of interest in the left hippocampus (CA1, CA2, CA2/3 CA3, DG) and four in the left cortex (S1, Pir, PLCo and PMCo). **(B)** Neuronal cell damage was evaluated in H&E staining exemplary for DG and PMCo comparing SAH vs. Sham surgery. Damaged neurons, characterized by hypereosinophilia, shrunken cytoplasm, and pyknotic nuclei, were software assisted counted and expressed as a ration to the total cell count per region.

Figure 4.

Neuronal cell loss. Cytomorphological quantification of neuronal damage at 6 (A), 24 (B) and 72 h (C) after SAH; given are mean and SD; * p<0.05; ** p<0.01; *** p<0.001; **** p<0.0001

Figure 5.

Microglial cell count. Counting of Iba-1 positive cells in five hippocampal, four cortical regions and the corpus callosum at 6 (A), 24 (B) and 72 h (C) after SAH; given are mean and SD; * p<0.05; ** p<0.01; *** p<0.001; **** p<0.0001

Additional Files

Table 1:

Neuronal damage 6 h after SAH

Neuronal damage 6 h after SAH: Demonstrated are the results for the hippocampal regions CA1, CA2, CA2/3, CA3 and DG and for the cortical regions S1, Pir, PLCo and PMCo; given are mean ranks (as Mann

Whitney U test was applied) and exact 2-sided p-values*Description of data

Table 2:

Neuronal damage 24 h after SAH

Neuronal damage 24 h after SAH: Demonstrated are the results for the hippocampal regions CA1, CA2, CA2/3, CA3 and DG and for the cortical regions S1, Pir, PLCo and PMCo; given are mean ranks (as Mann Whitney U test was applied) and exact 2-sided p-values

Table 3:

Neuronal damage 72 h after SAH

Neuronal damage 72 h after SAH: Demonstrated are the results for the hippocampal regions CA1, CA2, CA2/3, CA3 and DG and for the cortical regions S1, Pir, PLCo and PMCo; given are mean ranks (as Mann Whitney U test was applied) and exact 2-sided p-values

Table 4:

Microglial activation 6 h after SAH

Microglia activation 6 h after SAH: Demonstrated are the results for the hippocampal regions CA1, CA2, CA2/3, CA3 and DG and for the cortical regions S1, Pir, PLCo and PMCo and CC; given are mean ranks (as Mann Whitney U test was applied) and exact 2-sided p-values

Table 5:

Microglial activation 6 h after SAH

Microglia activation 24 h after SAH: Demonstrated are the results for the hippocampal regions CA1, CA2, CA2/3, CA3 and DG and for the cortical regions S1, Pir, PLCo and PMCo and CC; given are mean ranks (as Mann Whitney U test was applied) and exact 2-sided p-values

Table 6:

Microglial activation 6 h after SAH

Microglia activation 72 h after SAH: Demonstrated are the results for the hippocampal regions CA1, CA2, CA2/3, CA3 and DG and for the cortical regions S1, Pir, PLCo and PMCo and CC; given are mean ranks (as Mann Whitney U test was applied) and exact 2-sided p-values

Figures

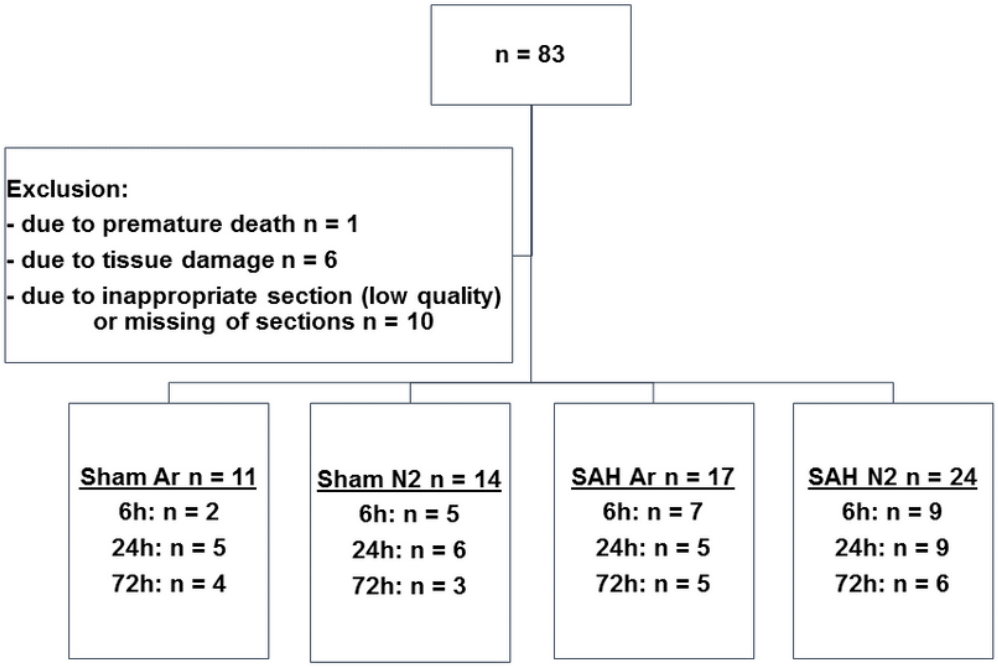

Figure 1

Flowchart of the animals included.

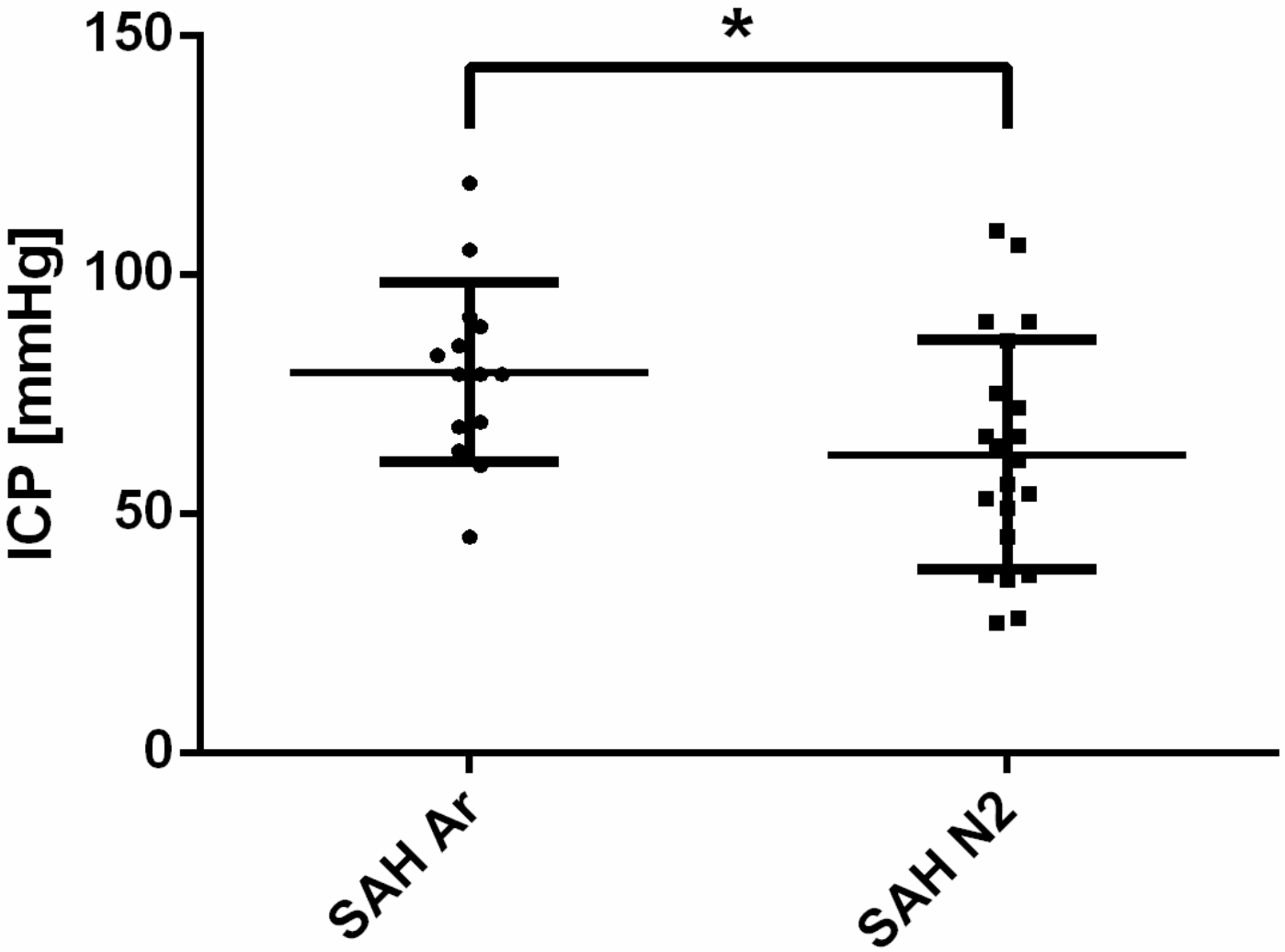

Figure 2

Peak ICP of the SAH treatment groups; given are mean and SD; * p<0.05

Figure 3

Selected regions of interest. (A) In H&E staining, a high power field was focused on five regions of interest in the left hippocampus (CA1, CA2, CA2/3 CA3, DG) and four in the left cortex (S1, Pir, PLCo and PMCo). (B) Neuronal cell damage was evaluated in H&E staining exemplary for DG and PMCo comparing SAH vs. Sham surgery. Damaged neurons, characterized by hypereosinophilia, shrunken cytoplasm, and pyknotic nuclei, were software assisted counted and expressed as a ration to the total cell count per region.

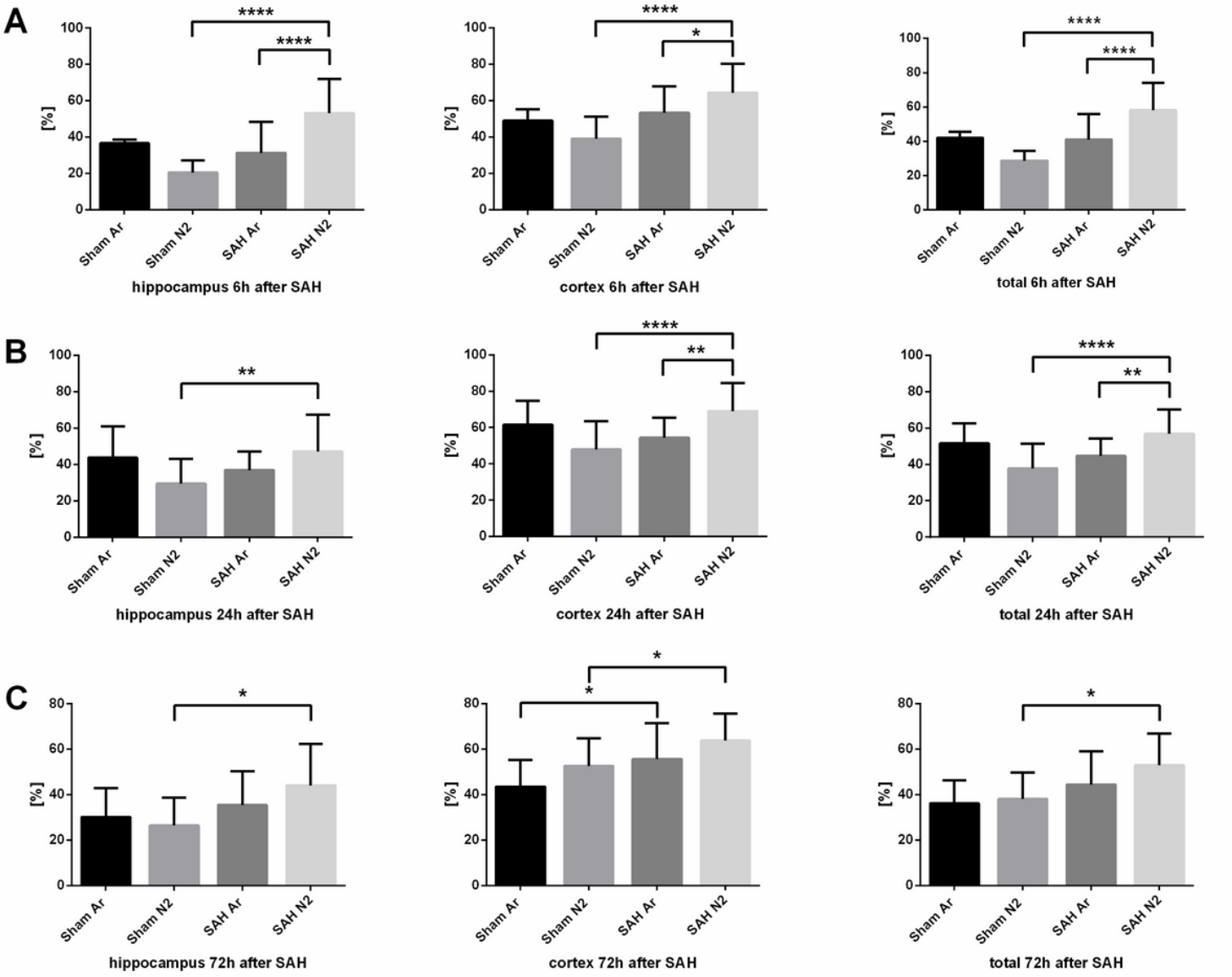

Figure 4

Neuronal cell loss. Cytomorphological quantification of neuronal damage at 6 (A), 24 (B) and 72 h (C) after SAH; given are mean and SD; * p<0.05; ** p<0.01; *** p<0.001; **** p<0.0001

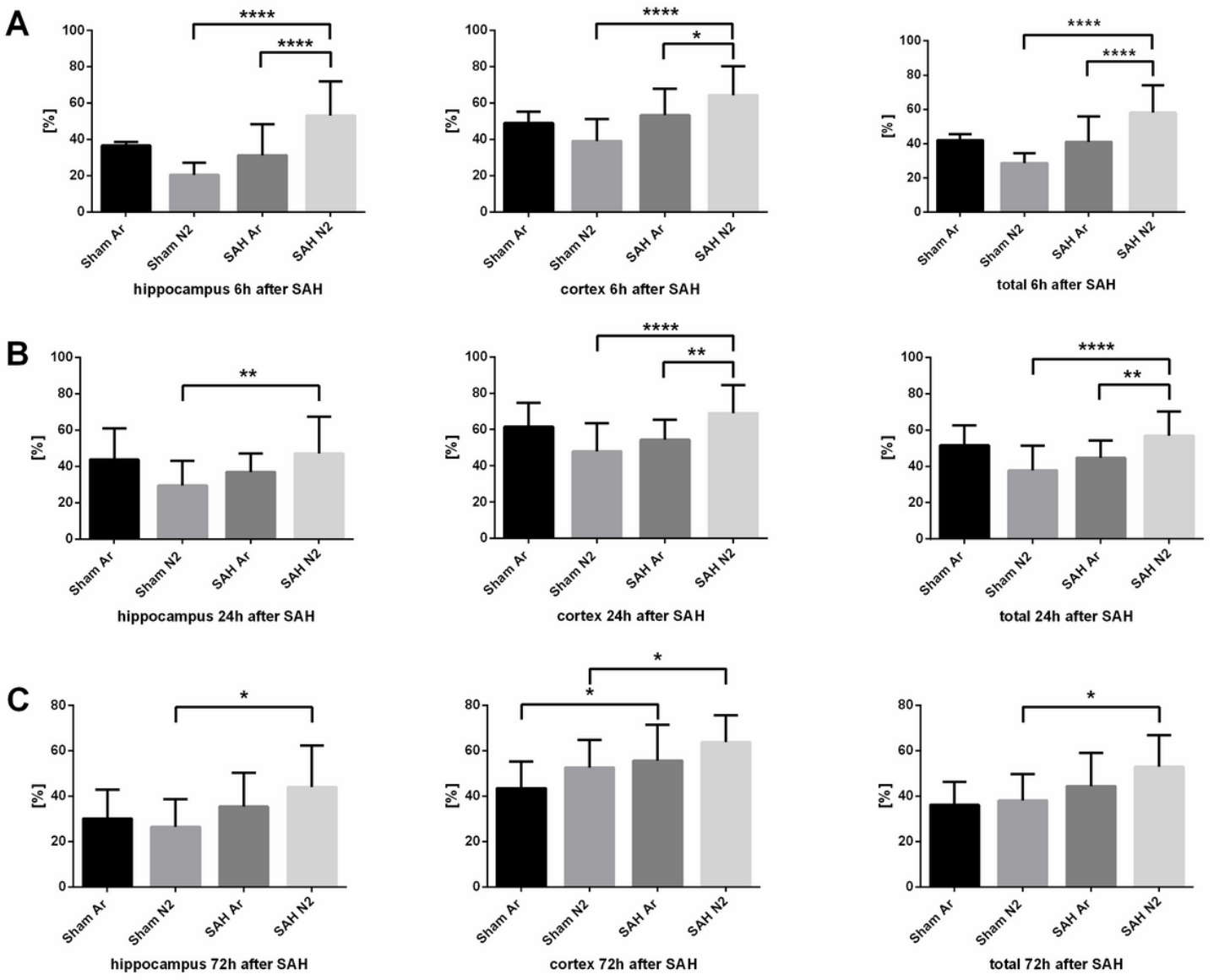

Figure 5

Microglial cell count. Counting of Iba-1 positive cells in five hippocampal, four cortical regions and the corpus callosum at 6 (A), 24 (B) and 72 h (C) after SAH; given are mean and SD; * p<0.05; ** p<0.01; *** p<0.001; **** p<0.0001

Supplementary Files

This is a list of supplementary files associated with this preprint. Click to download.

- Table6MG72hafterSAH.pdf
- NC3RsARRIVEGuidelinesChecklistfillableBK.pdf
- Table4MG6hafterSAH.pdf

- Table3neuronaldamage72hafterSAH.pdf
- Table5MG24hafterSAH.pdf
- Table1neuronaldamage6hafterSAH.pdf
- Table2neuronaldamage24hafterSAH.pdf